Influence of building block aromaticity in the determination of electronic properties of five-membered heterocyclic oligomers

David Delaere, Minh Tho Nguyen* and Luc G. Vanquickenborne

Department of Chemistry, University of Leuven, Celestijnenlaan 200F, B-3001 Leuven, Belgium. E-mail: minh.nguyen@chem.kuleuven.ac.be

This theoretical study investigates the influence of the building block aromaticity in the determination of electronic properties of five-membered heterocyclic oligomers. More specifically, we considered some fundamental energetic and electronic properties such as energy gaps, vertical ionization energies and static polarizability tensors of oligomers (up to octamers) built from five-membered heterocycles such as cyclopentadiene, pyrrole, furan, silole, (planar) phosphole and thiophene. Our computations are based on *ab initio* quantum mechanical methods including (time-dependent) density functional theory. We have chosen NICS as a quantitative criterion for measuring aromaticity and making a distinction between aromatic and non-aromatic building blocks.

Introduction

Organic heterocyclic oligomers and polymers based on thiophene or pyrrole derivatives have attracted much attention during the last decade owing to their interesting electrical and/or (nonlinear) optical properties.[1] Relatively little is known about the oligomers derived from analoguous five-membered rings such as cyclopentadiene, furan, silole and phosphole; this is mainly due to the experimental difficulties in their syntheses.

Yet, poly(2,5)siloles which were proposed more than a decade ago,[2] have been quite recently synthesized for the first time.[3] Mathey and coworkers[4a–d] and Réau and coworkers[4e,f] have been attempting to design efficient routes to prepare a variety of phosphole oligomers that are the first necessary steps toward phosphole polymers.

It has widely been recognized for polyconjugated polymers that, besides the morphology problems, their chemical and structural defects make a deeper understanding of the origin of a given property more arduous. As a consequence, comparison between experimental and theoretical results is a very difficult task for polymers. On the contrary, oligomers represent ideal systems for a theoretical study based on *ab initio* quantum chemical methods since their properties are intrinsically associated with those of an isolated chain and affected only slightly by the environment. Furthermore, a thorough understanding of the electronic properties of well-defined oligomers provides us with a good basis for unraveling those properties in the more complex polymers. Therefore, we have chosen to focus particular attention on the oligomeric systems.

In this paper, we report the results of an investigation on the influence of the aromaticity of the building blocks in determining some fundamental energetic and electronic properties of the oligomers, more specifically, the energy gaps, vertical ionization energies and static dipole polarizabilities of oligomers built from five-membered heterocycles such as cyclopentadiene, pyrrole, furan, silole, (planar) phosphole and thiophene. The more specific influence of the heteroatom or bridging group on those electronic properties has been considered in earlier theoretical studies.[5–9]

The present paper is organized as follows: first, we will consider the molecular and electronic structure of the monomers (building blocks). Subsequently, we will describe the geometry of the oligomer structures and compare the competition between linear- and cyclic π-conjugation in oligomers built from aromatic *versus* non-aromatic five-membered heterocycles. Finally, we will discuss how the building block aromaticity influences the energy gaps and the static polarizability tensors.

Computational details

Methods

Density functional theory (DFT)[10] was employed in order to carry out geometry optimizations, natural bond orbital (NBO) analysis, and to compute static polarizability tensors.

The lower-lying excited states arising from HOMO→LUMO transitions were treated within the adiabatic approximation of *time dependent density functional theory* (TDDFT).[11] All DFT-calculations were performed using the three-parameter Lee–Yang–Parr (B3LYP) functional in conjunction with the split valence plus polarization SV(P)[12] or 6-31G*[13] basis sets. Both basis sets have comparable quality. The hybrid B3LYP functional constitutes a considerable improvement over Hartree–Fock approaches and yields good performance in calculating static polarizability tensors[14] and low-lying electronic excitations.[11]

The *Hartree–Fock* (HF) approach was used to evaluate nucleus-independent chemical shifts[15] (NICS) and vertical ionization energies (IEs). NICS-values were computed making use of the GIAO-HF/6-311G* method. IEs were obtained from negative HOMO-energies (Koopmans' theorem) using the HF/SV(P) method. At the HF level, correlation effects tend to cancel the relaxation error and reasonable first approximations to experimental ionzation energies are obtained.[16]

Table 1 Overview of heterocyclic building blocks used in this work

		X	NICS (ppm)	Aromaticity
		First row		
Cyclopentadiene	Cp	CH_2	−4.8	Non-aromatic
Pyrrole	Py	NH	−16.0	Aromatic
Furan	Fu	O	−13.2	Aromatic
		Second row		
Silole	Si	SiH_2	+0.3	Non-aromatic
Phosphole	Ph	PH	−5.5	Non-aromatic
Planar phosphole	Pl Ph	PH	−18.4	Aromatic
Thiophene	Th	S	−14.6	Aromatic

π-Conjugation analysis

As shown in our previous study on phosphole monomers,[17] *combination of both geometric (Julg index) and magnetic (NICS) criteria* leads to an interesting approach to analyze the π-electron delocalization in conjugated heterocyclic systems. Since we are considering oligomers, the *interring bond distances ($d_{C\alpha}$)* are also taken into account in order to reflect the strength of π-electron conjugation between neighboring repeat units.

The *Julg index*,†[18,19] referred to hereafter as JI, is defined in terms of the deviations of the individual C–C bond lengths (r_i) from the mean carbon–carbon bond length (r) and constitutes a measure of the bond length alternation (π-electron conjugation) in the 1,3-butadienic unit. The π-conjugation along the 1,3-butadiene unit will be more pronounced if the JI becomes closer to one. The JI is influenced by the aromaticity of the considered heterocycle and by the linear π-conjugation towards the neighboring repeat units. In the *nucleus-independent chemical shift-approach*,[15] the absolute magnetic shieldings are computed at the ring centre (nonweighted mean of the heavy atom coordinates). With respect to the familiar NMR chemical shift convention, the sign of the computed values are reversed: negative NICS-values denote aromaticity. The more negative the NICS value, the more aromatic the system. As a reference point, we would like to mention the NICS value for benzene, which amounts to −10.5 ppm at HF/6-311G* level.

Conjugation effects were also analysed in terms of localized orbitals constructed within the NBO method, which is based on natural population analysis.[20] The essential feature of *NBO analysis* is that the electron density is represented, as far as possible, by localized core orbitals, bonds, and lone-pairs. These orbitals are related to Lewis structures corresponding to the chemist's view of molecules built from atoms connected by localized two-electron bonds. However, for conjugated systems, ideal Lewis structures are obviously not adequate. Deviations from idealized Lewis structures due to conjugation are shown in NBO analysis as orbital interactions between localized bonds and anti-bonds and between lone-pairs and anti-bonds. The energetic contributions from these interactions can be quantified with the help of second-order perturbation theory [eqn. (1)].

$$E^{(2)} = n \frac{\langle F_{ij} \rangle^2}{\varepsilon_{ij}} \tag{1}$$

Where $E^{(2)}$ is the second-order perturbational energy stabilization; F_{ij} is the Fock matrix element between occupied orbital *i* and unoccupied orbital *j* and can be taken to be proportional to the overlap between those orbitals; ε_{ij} is the energy difference between orbitals *i* and *j*, and *n* is the occupancy of orbital *i*. Since perturbation theory is only valid for small perturbations, absolute stabilizations become less reliable as their values increase. Therefore, we do not attach too much importance to the absolute values of stabilization energies but we are more concerned with the general trends.

Programs

The Turbomole program[12] was employed for optimizing molecular geometries and calculating energy gaps, vertical ionization energies and static polarizability tensors. The Gaussian 98 program[13] was used for carrying out NBO-analysis and computing NICS-values.

Results and discussion

Structures

Monomers. All monomer units described in this work (apart from 1,3-butadiene) are heterocyclic five-membered rings. Their structures are planar, except for phosphole that contains a pyramidal tri-coordinated phosphorus atom which prevents efficient interaction of the phosphorus lone-pair with the 1,3-butadiene unit. Planar phosphole was considered as a hypothetical structure. Each monomer can be seen as a combination of a 1,3-butadiene system with a first- or second row heteroatom (Table 1). The interaction between the heteroatom and the 1,3-butadiene unit is different for each heterocycle and will determine whether the building block is aromatic or not. Aromatic heterocycles are characterized by a strong cyclic π-conjugation, which induces a significant diamagnetic ring current. We have chosen NICS as a quantitative criterion for measuring this ring current. By doing this, we were able to distinguish aromatic and non-aromatic building blocks. Cyclopentadiene (Cp), silole (Si) and phosphole (Ph) possess a NICS value of −4.8, +0.3 and −5.5 ppm, respectively, which is much more positive than the −10.5 ppm of benzene and points out those heterocycles are not characterized by a significant cyclic π-conjugation or can be classified as non-aromatic. On the other hand, pyrrole (Py), furan (Fu), planar phosphole (Pl Ph) and thiophene (Th) possess a NICS value of −16.0, −13.2, −18.4 and −14.6 ppm, respectively, which is more negative than that of benzene and proves those heterocycles are characterized by strong cyclic π-conjugation and can be classified as aromatic building blocks. Since NICS is a quantitative criterion, we can conclude that furan has the lowest cyclic π-conjugation within the aromatic heterocycles.

To compare the electronic structure of the considered building blocks we have drawn orbital correlation diagrams for their π-valence orbitals. These diagrams are presented in Fig. 1. The HOMO and LUMO orbitals of the considered building

† JI = $1 - (225/n)\sum(1 - r_i/r)^2$, $n = 3$ and represents the number of C–C bonds. JI = 1 for benzene (D_{6h}) and the cyclopentadienyl ion (D_{5h}), that is, for the fully delocalized, highest symmetric systems. The empirical factor 225 provides an aromaticity scale in which JI = 0 for the Kekulé form of benzene (assuming 1.33 and 1.52 Å C–C lengths).
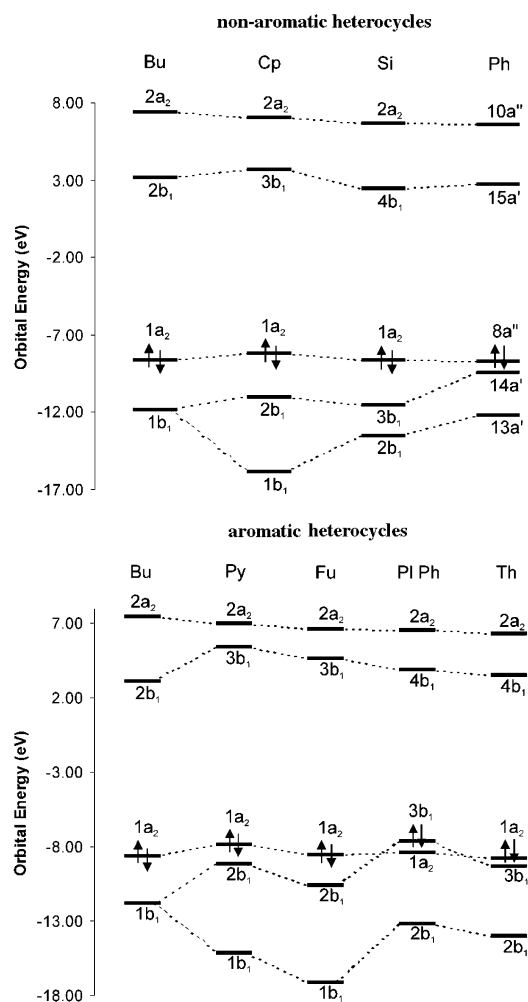
Fig. 1 Orbital correlation diagrams for the π-valence orbitals of the considered building blocks at HF/6-31G* level.

blocks are drawn in Figs. 2 and 3. Aromatic and non-aromatic heterocycles are considered seperately in Figs. 1–3.

The valence orbitals are labelled as b_1 or a' and a_2 or a'' for heterocycles characterized by C_{2v} or C_s symmetry, respectively. The orbital π-valence structure for 1,3-butadiene which is composed of two π bonding and two π* anti-bonding orbitals, is drawn on the left side in both correlation diagrams (Fig. 1).
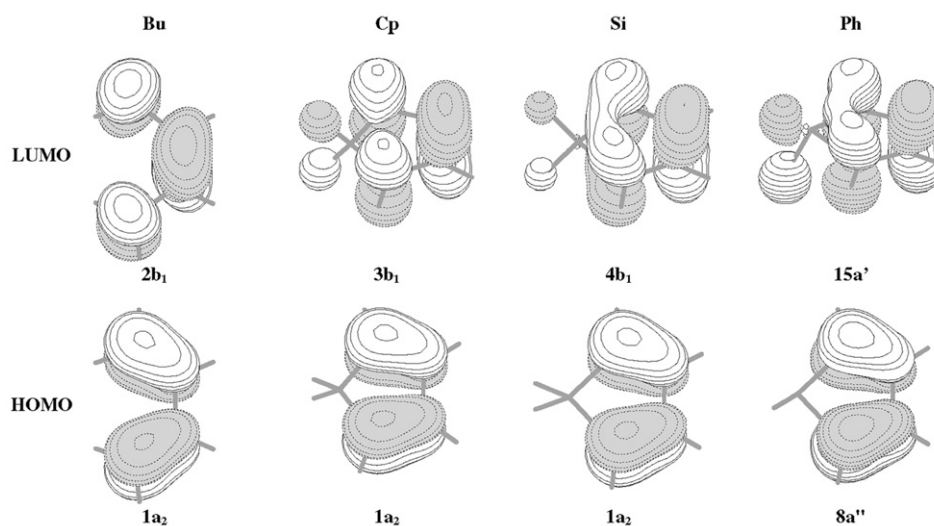
Figs. 2 and 3 show that the b_1 or a' representation allow interactions between the heteroatom and π-valence structure of 1,3-butadiene; the a_2 or a'' representation does not.

Since properties such as vertical ionization energies (IE) and energy gaps (E_g) are related to the frontier orbital energies, it is instructive to have a closer look at the HOMO and LUMO orbitals. All but one HOMOs have a_2 or a'' symmetry and resemble the 1,3-butadiene HOMO ($1a_2$). The Pl Ph HOMO ($3b_1$) (Fig. 3) forms the only exception, and is built from the lowest π-bonding 1,3-butadiene orbital ($1b_1$) in anti-bonding interaction with the phosphorus lone-pair (n_P). All LUMOs have b_1 or a' symmetry and can been seen as the result of the interaction between the 1,3-butadiene π*($2b_1$) orbital and the lone-pair n_X and/or σ_{X-H} orbitals of the heteroatom. As illustrated in Fig. 3 and quantified in Table 2, the aromatic heterocycles are characterized by a lone pair orbital (n_X) on the heteroatom X that strongly interacts with the π*(b_1) orbitals and whereby the interaction between the heteroatom and the π-butadiene unit is stronger for first row heteroatoms (N, O) as compared with second row ones (P, S). The reason is that the n_X orbitals of first row heteroatoms have better overlap with the butadiene π-valence orbitals as compared with the second row atom n_X orbitals. On the other hand, the non-aromatic heterocycles[7,21] are characterized by weaker orbital interactions between the heteroatom (lone-pair or exocyclic σ_{X-H} bonds) and the butadiene π*(b_1) orbitals, which is illustrated in Fig. 2 and also quantified in Table 2. As a consequence and as shown in Fig. 1, the LUMO orbitals are more destabilized for the aromatic heterocycles compared to the non-aromatic counterparts.

Oligomers. The geometries of α-linked oligomers of 1,3-butadiene, cyclopentadiene, pyrrole, furan, silole, (planar) phosphole and thiophene were optimized up to octamers. The repeat units were *trans*-oriented and kept coplanar. Except for phosphole, all structures containing an odd number of repeat units have C_{2v} symmetry; the ones comprising an even number of repeat units have C_{2h} symmetry. Phosphole oligomers containing an odd number of repeat units are characterized by C_s symmetry; for an even number of repeat units the symmetry is C_2. Each ring of a heterocyclic oligomer can be characterized by a JI and a NICS value. The π-conjugation along the 1,3-butadiene unit of that ring will be more pronounced if the JI becomes closer to one and the heterocyclic five-membered ring will be more aromatic (stronger cyclic π-conjugation) if the NICS value becomes more negative. Whereas, the shorter the interring bond distance ($d_{C\alpha}$), the

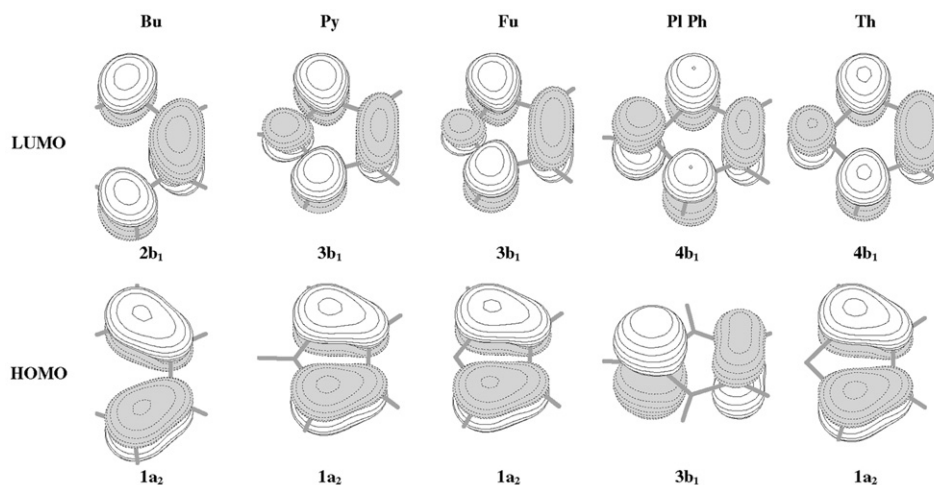**Fig. 2** Frontier orbitals of 1,3-butadiene and non-aromatic heterocycles at HF/6-31G* level.

Fig. 3 Frontier orbitals of 1,3-butadiene and aromatic heterocycles at HF/6-31G* level.

more pronounced the linear π-conjugation between neighboring repeat units.

Julg indices, NICS- and $d_{C\alpha}$-values of α-linked tetramers are presented in Table 3. These results reflect the trends observed in all α-linked oligomers considered, going from trimers to octamers.

They show the JIs for the inner rings are larger than those for the outer rings and that the $d_{C\alpha}$-values between inner rings are smaller than those between outer rings, which clearly indicates a more pronounced linear π-conjugation between inner rings than between outer rings. Moreover, the cyclic π-conjugation becomes smaller in the inner rings as proven by their more positive NICS-values.

From Table 3 it is also clear that the $d_{C\alpha}$-values are shorter in oligomers made from non-aromatic building blocks as compared to oligomers built up from aromatic building blocks. Therefore, it can be concluded that the linear π-conjugation is more pronounced in non-aromatic heterocyclic oligomers. Fu-oligomers are an exception to the rule. The NBO-analysis on trimers, presented in Table 2, confirms this finding. For non-aromatic oligomers the $\pi_{C1C2} \rightarrow \pi^*_{C1'C2'}$ interactions are larger than for $\pi_{C1C2} \rightarrow \pi^*_{C3C4}$, which points out that π-elec-

trons in the central 1,3-butadiene unit tend to be more delocalized toward the outer rings than to stay within that central ring. For aromatic heterocyclic oligomers the reverse situation is true, but again, furan oligomers are found to be an exception.

Electronic properties

Energy gaps and ionization energies. The energy gap (E_g) represents the difference in energy between both the highest occupied molecular orbital (HOMO) and lowest unoccupied molecular orbital (LUMO) and was determined in this work by computing the minimum electronic excitation energy using TDDFT. For π-conjugated systems such as polyenes and the heterocyclic π-conjugated oligomers considered here, the lowest allowed excitations correspond with singlet $\pi^* \leftarrow \pi$ transitions and provide an estimate for λ_{max} in the UV/VIS absorption spectra.

Within the framework of HF theory and Koopman's theorem the negative of the HOMO energy (ε_{HOMO}) corresponds to the vertical ionization energy (IE).

Table 2 Strength of $\pi \rightarrow \pi^*$, $n_X \rightarrow \pi^*$ and $\sigma_{X-H} \rightarrow \pi^*_{C1C2}$ interactions out of an NBO-analysis on trimers at B3LYP/6-31G* level

Non-aromatic building blocks		E/kJ mol^{-1}	Aromatic building blocks		E/kJ mol^{-1}	F_{ij} (a.u.)
Bu (no X)	$\pi_{C1C2} \rightarrow \pi^*_{C1'C2'}$	71.09	Py	$\pi_{C1C2} \rightarrow \pi^*_{C1'C2'}$	65.48	
	$\pi_{C1'C2'} \rightarrow \pi^*_{C1C2}$	71.13		$\pi_{C1'C2'} \rightarrow \pi^*_{C1C2}$	66.44	
	$\pi_{C1C2} \rightarrow \pi^*_{C3C4}$	62.88		$\pi_{C1C2} \rightarrow \pi^*_{C3C4}$	75.77	
				$n_N \rightarrow \pi^*_{C1C2}$	162.34	0.095
Cp	$\pi_{C1C2} \rightarrow \pi^*_{C1'C2'}$	74.56	Fu	$\pi_{C1C2} \rightarrow \pi^*_{C1'C2'}$	68.03	
	$\pi_{C1'C2'} \rightarrow \pi^*_{C1C2}$	73.47		$\pi_{C1'C2'} \rightarrow \pi^*_{C1C2}$	67.24	
	$\pi_{C1C2} \rightarrow \pi^*_{C3C4}$	67.40		$\pi_{C1C2} \rightarrow \pi^*_{C3C4}$	65.86	
	$\sigma_{C-H} \rightarrow \pi^*_{C1C2}$	2.96		$n_O \rightarrow \pi^*_{C1C2}$	115.39	0.091
Si	$\pi_{C1C2} \rightarrow \pi^*_{C1'C2'}$	69.54	Th	$\pi_{C1C2} \rightarrow \pi^*_{C1'C2'}$	61.59	
	$\pi_{C1'C2'} \rightarrow \pi^*_{C1C2}$	69.28		$\pi_{C1'C2'} \rightarrow \pi^*_{C1C2}$	61.46	
	$\pi_{C1C2} \rightarrow \pi^*_{C3C4}$	63.09		$\pi_{C1C2} \rightarrow \pi^*_{C3C4}$	68.07	
	$\sigma_{Si-H} \rightarrow \pi^*_{C1C2}$	0.98		$n_S \rightarrow \pi^*_{C1C2}$	87.65	0.067
Ph	$\pi_{C1C2} \rightarrow \pi^*_{C1'C2'}$	67.57	Pl Ph	$\pi_{C1C2} \rightarrow \pi^*_{C1'C2'}$	59.54	
	$\pi_{C1'C2'} \rightarrow \pi^*_{C1C2}$	66.40		$\pi_{C1'C2'} \rightarrow \pi^*_{C1C2}$	59.16	
	$\pi_{C1C2} \rightarrow \pi^*_{C3C4}$	64.35		$\pi_{C1C2} \rightarrow \pi^*_{C3C4}$	76.52	
	$n_p \rightarrow \pi^*_{C1C2}$	12.72		$n_p \rightarrow \pi^*_{C1C2}$	110.42	0.067
	$\sigma_{P-H} \rightarrow \pi^*_{C1C2}$	2.25				

Table 3 Julg indices, NICS (ppm) and $d_{C\alpha}$ (Å) values for α-linked tetramers

Building blocks	JI		NICS		$d_{C\alpha}$	
	Inner	Outer	Inner	Outer	Inner	Outer
Non-aromatic						
Bu	0.86	0.72			1.432	1.436
Cp	0.86	0.76	−0.8	−2.2	1.434	1.439
Si	0.85	0.71	+1.7	+1.3	1.435	1.440
Ph	0.92	0.83	−2.7	−4.0	1.437	1.442
Aromatic						
Py	0.99	0.97	−13.2	−14.6	1.447	1.449
Fu	0.94	0.90	−10.8	−11.9	1.435	1.439
Pl Ph	1.00	0.99	−15.1	−16.7	1.447	1.449
Th	0.97	0.94	−10.8	−12.6	1.446	1.450

Computed energy gaps and vertical ionization energies are tabulated in Tables 4 and 5 for non-aromatic and aromatic heterocyclic oligomers, respectively. Experimental E_g and IE are given where available.

Zotti *et al.*[22] performed UV/VIS spectroscopic studies at room temperature for a number of pyrrole oligomers, denoted hereafter as py1, py2, py3, py5 and py7, in acetonitrile (polar aprotic solvent). Birnbaum and Kohler[23–25] carried out highly resolved spectral investigations on thiophene oligomers (th2–th4) in hexane and decane (non-polar solvents) at low temperature. Stationary absorption and fluorescence spectra for thiophene oligomers (th2–th6) in dioxane (non-polar solvent) were measured at room temperature by Colditz *et al.*[26] UV/VIS absorption measurements were carried out on hexathiophene (th6) single crystals grown from the vapor phase by Horowitz *et al.*[27] Salzner *et al.*[28] computed vertical excitation energies of medium sized and large pyrrole and thiophene oligomers using DFT /hybrid functionals that included 30% HF exchange. The energy gaps were determined by simply taking the differences in energy between HOMO and LUMO energy levels.

Since measured energy gaps at both low and room temperature were only found for thiophene oligomers, we focused on these data to calibrate the accuracy of our TDDFT results. As mentioned before, calculations were performed on *trans*-oriented co-planar oligomers in the gas phase. Expecting the results in non-polar solvent to be 0.2–0.3 eV lower than in the gas-phase,[28] our TDDFT results are within 0.2 eV of experimental low-temperature energy gaps, whereas the energy gaps calculated by Salzner *et al.*[28] differ by more than 0.5 eV. The energy gaps for thiophene oligomers measured at room temperature are around 0.4 eV higher in energy than those measured at low-temperature. This larger discrepancy is probably due to the larger distortions of the conjugated system at room temperature. The measured energy gap for *trans* co-planar hexathiophene performed in gas phase at room temperature by Horowitz *et al.*[27] is in good agreement with our computed energy gap and supports above supposition.

Comparison between experimental and theoretical IEs for Py monomers[29] and Th monomers[30] and dimers[31] shows that IEs are reasonably well predicted at HF level using Koopman's theorem.

The dependence of HOMO and LUMO ortibal energies (ε_{HOMO}, ε_{LUMO}) on the chain-length n_c (number of carbon atoms) is presented in Fig. 4, which shows that ε_{HOMO} rises and ε_{LUMO} lowers as the chain length increases. As a consequence, both E_g and IE decrease with increasing chain length, which is shown in Fig. 5. By the octamers ($n_c = 32$), both ε_{HOMO}- and ε_{LUMO}-values and the related properties E_g and IE appear to be levelling off, irrespective of whether the building blocks are aromatic or not. The ordering of the considered π-conjugated octamers according to increasing energy gap is computed as follows: Si: 1.4 eV < Ph = Cp = Bu: 1.6 eV ≪ Th: 2.2 eV < Pl Ph: 2.4 eV < Fu: 2.5 eV < Py: 2.8 eV

Table 4 Computed energy gaps (E_g) at B3LYP/SV(P) level and vertical ionization energies (IE) at HF/SV(P) level for non-aromatic heterocyclic oligomers

Oligomer	E_g/eV	IE/eV	Oligomer	E_g/eV	IE/eV
Bu			*Cp*		
bu1	5.4	8.8	cp1	5.1	8.4
bu2	3.8	7.5	cp2	3.5	7.1
bu3	3.0	6.9	cp3	2.8	6.5
bu4	2.5	6.6	cp4	2.3	6.1
bu5	2.2	6.3	cp5	2.1	5.9
bu6	1.9	6.2	cp6	1.9 (1.8)[a]	5.8
bu7	1.7	6.1	cp7	1.7	5.7
bu8	1.6	6.0	cp8	1.6	5.6
Si			*Ph*		
si1	4.4	8.9	ph1	4.7	8.9
si2	3.2	7.6	ph2	3.3	7.6
si3	2.5	7.0	ph3	2.7	7.0
si4	2.1	6.7	ph4	2.3	6.7
si5	1.9	6.5	ph5	2.0	6.5
si6	1.7 (2.1)	6.3	ph6	1.8 (1.9)	6.4
si7	1.5	6.2	ph7	1.7	6.3
si8	1.4	6.1	ph8	1.6	6.2

[a] The oscillator strengths (a.u.) for heterocyclic hexamers are given in brackets.

Table 5 Computed energy gaps (E_g) at B3LYP/SV(P) level and vertical ionization energies (IE) at HF/SV(P) level for aromatic heterocyclic oligomers

Oligomer	E_g/eV Theor. Own		Expt. Room T.	IE/eV Theor. Own	Expt.	Oligomer	E_g/eV Theor. Own		Expt. Low T.	Expt. Room T.	IE/eV Theor. Own	Expt.
Py						*Fu*						
py1	6.7	7.44[a]	5.96[b]	8.1	8.21[h]	fu1	6.5				8.8	
py2	4.7	5.49[a]	4.49[b]	6.9		fu2	4.6				7.5	
py3	3.9	4.73[a]	3.91[b]	6.3		fu3	3.7				7.0	
py4	3.5	4.34[a]		6.1		fu4	3.2				6.7	
py5	3.2	4.10[a]	3.38[b]	5.9		fu5	2.9				6.5	
py6	3.0 (1.9)[k]	3.95[a]		5.8		fu6	2.7 (1.9)				6.4	
py7	2.9		3.26[b]	5.7		fu7	2.6				6.4	
py8	2.8			5.7		fu8	2.5				6.3	
Pl Ph						*Th*						
plph1	5.3			7.8		th1	5.9	6.73[a]			9.0	8.85[i]
plph2	4.1			7.2		th2	4.0	4.80[a]	3.66[c]	4.05[g]	7.7	7.63[j]
plph3	3.4			6.6		th3	3.3	4.00[a]	3.06–3.07[d]	3.49[g]	7.2	
plph4	3.0			6.4		th4	2.9	3.58[a]	2.74–2.75[e]	3.16[g]	6.9	
plph5	2.8			6.2		th5	2.6	3.32[a]		2.99[g]	6.7	
plph6	2.6 (2.1)			6.1		th6	2.4 (2.0)	3.15[a]		2.41[f] 2.85[g]	6.6	
plph7	2.5			6.1		th7	2.3				6.6	
plph8	2.4			6.0		th8	2.2				6.5	

[a] Ref. 28. [b] Ref. 22. [c] Ref. 23. [d] Ref. 24. [e] Ref. 25. [f] Ref. 27. [g] Ref. 26. [h] Ref. 29. [i] Ref. 30. [j] Ref. 31. [k] The oscillator strengths (a.u.) for heterocyclic hexamers are given in brackets.

and agree with the ordering according to increasing band gap found by Salzner *et al.*[6] for the corresponding polymers. The energy gaps are smaller for octamers built up from non-aromatic building blocks, since their LUMOs (Fig. 4) are more stable as compared to those of their aromatic counterparts (see the section entitled Monomers).

The HOMOs aren't influenced by the building block aromaticity (Fig. 4). Therefore, no correlation is expected between the vertical ionization energy and the building block aromaticity. Through the series of considered heterocyclic oligomers, we observe that Cp- and Py-oligomers have the lowest IEs,

ranging from 8.1–8.4 eV in the momoners to 5.6–5.7 eV in the octamers. The IEs for Fu-, Si-, Ph- and Th-oligomers are higher and range from 8.8–9.0 eV in the momoners to 6.1–6.5 eV in the octamers. Remarkably, planar phosphole oligomers (Pl Ph) have lower IEs than the corresponding phosphole oligomers (Ph). Flattening the pyramidal phosphorus atom allows stronger anti-bonding interaction between n_P and the $\pi(b_1)$ 1,3-butadiene orbital. This raises the HOMO-1 orbital for Ph by around 1.8 eV at HF/6-31G*s level towards the corresponding HOMO orbital for Pl Ph,[32, 33] which lies about 1.0 eV higher than the HOMO orbital for Ph. The IE for Pl Ph
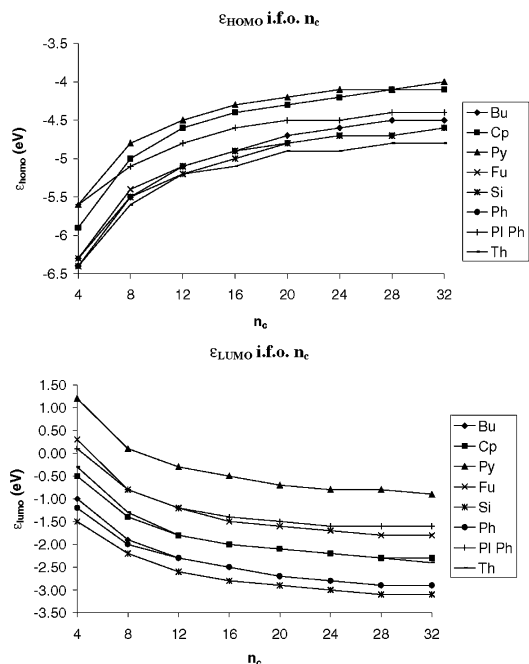
Fig. 4 Chain-length dependence of ε_{HOMO} and ε_{LUMO} at B3LYP/SV(P) level.
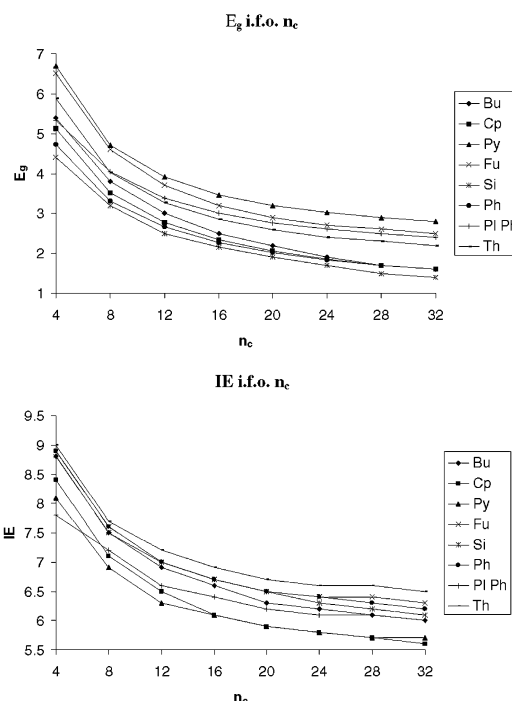
Fig. 5 Chain-length dependence of E_g at B3LYP/SV(P) level and IE at HF/SV(P) level.

amounts to 7.8 eV. The HOMO orbital for Ph resembles the 1,3-butadiene HOMO and corresponds to the HOMO-1 orbital for Pl Ph—both have similar energy. The IE for Ph is computed at 8.9 eV.

For the phosphole dimer the difference in HOMO energy between planar and puckered phosphole is significantly reduced. In fact, they have now both in common the 1,3-butadiene HOMO. The HOMO of the planar phosphole still has some phosphorus n_P-contribution, responsible for lowering the IE by 0.4 eV. But the contribution of the phosphorus lone-pair orbital to the HOMO orbital decreases with increasing chain length. For the octamers the difference in IEs between both structures built from planar and puckered phosphole units amounts to only 0.2 eV. The IEs for Pl Ph and Ph octamers amount to 6.0 and 6.2 eV, respectively.

Static polarizability tensors. When a molecule is placed in an external electrostatic field F, molecular charge reorganization causes the dipole moment to change. Eqn. (2) gives the linear response of μ towards F

$$\mu = \mu_0 + \alpha \cdot F \qquad (2)$$

where μ_0 is the permanent electric dipole moment. The static polarizability α, describes the charge distribution deformability under the action of an external electrostatic field F and is of great importance in the area of intermolecular forces and opto-electronics. The explicit formula for α is given in eqn. (3).

$$\alpha = \frac{2}{3} \sum_n \frac{|\langle 0|\mu|n\rangle|^2}{E_n - E_0} \qquad (3)$$

The property α is characterized as a second rank tensor. We investigated the influence of the building block aromaticity on the static polarizability tensors. The quantities reported hereafter are the average polarizability $\langle\alpha\rangle$ [eqn. (4)] and the polarizability anisotropy $\Delta\alpha$ [eqn. (5)]

$$\langle\alpha\rangle = 1/3(\alpha_{xx} + \alpha_{yy} + \alpha_{zz}) \qquad (4)$$

$$\Delta\alpha = \{1/2[(\alpha_{xx} - \alpha_{yy})^2 + (\alpha_{xx} - \alpha_{zz})^2 + (\alpha_{yy} - \alpha_{zz})^2]\}^{1/2} \qquad (5)$$

where $\alpha_{ii}(i = x, y \text{ or } z)$ are the diagonal elements of the polarizability tensor.

It is important to note that we have only computed the static electronic contributions to the polarizability, the frequency dependent character of the polarizability was not taken into account. Calculations were performed on oligomers placed in the yz plane, with chain length increasing along the y-axis (longitudinal direction), as shown in Fig. 6. The static polarizabilities are expressed in 10^{-40} C V^{-1} m^2 units.

Experimental and computed average polarizabilities $\langle\alpha\rangle$ for thiophene oligomers are recorded in Table 6, which highlights the large frequency dependence of the $\langle\alpha\rangle$-values. Champagne *et al.*[34] calculated the average polarizabilities extrapolated to zero frequency $\langle\alpha\rangle_{\lambda=\infty}$ based on experimental results of Zhao *et al.*[35] who measured the refractive indices of thiophene oligomers in THF solution at the wavelength of the sodium D line ($\lambda = 589$ nm) and subsequently evaluated the polarizabilities.

The chain-length dependence of the computed and extrapolated experimental $\langle\alpha\rangle$-values per unit cell ($\langle\alpha\rangle/n$) at the static limit were plotted in Fig. 7. We note that the deviation between both values becomes significant from tetramers on and further rises dramatically going to hexamers. In search for an explanation for this deviation, we started wondering about the long chain behavior of both computed and extrapolated $\langle\alpha\rangle$-values.

On the one hand, we found in the literature[36] that the DFT/B3LYP method is in trouble when dealing with linear and non-linear responses of extended systems. But these errors should lead to an overestimate of α, which is in the opposite direction
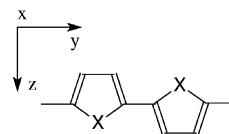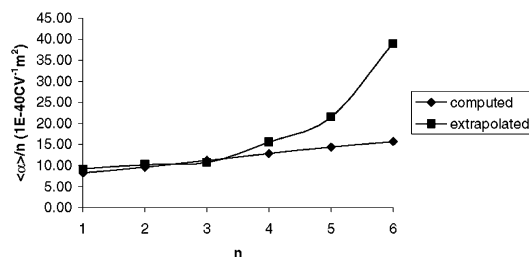
Fig. 6 The oligomer orientation used for determining polarizability tensors.

Table 6 Average polarizability $\langle\alpha\rangle$ of thiophene oligomers expressed in 10^{-40} C V^{-1} m^2

Th	$\langle\alpha\rangle_{\text{Theor.}}$	$\langle\alpha\rangle_{\lambda=589 \text{ nm}}$[a]	$\langle\alpha\rangle_{\lambda=\infty}$[b]
		$\langle\alpha\rangle_{\text{Expt.}}$	
th1	8.3	10.9	9.2
th2	19.3	27.8	20.5
th3	33.7	50.1	32.3
th4	51.6	111.4	62.3
th5	72.1	211.7	107.5
th6	94.6	501.3	233.8

[a] Ref. 37. [b] Ref. 36.

Fig. 7 Chain-length dependence of computed and extrapolated $\langle\alpha\rangle/n$ values at the static limit.

to the deviation we have found. Furthermore, if we compare our DFT- with SCF-results obtained by Luo *et al.*,[37] we observe the same trend with both methods. The $\langle\alpha\rangle/n$ value first increases with the size of the system and seems to saturate around 9 repeat units. On the other hand, the extrapolation model[34] for defining static average polarizabilities using experimental $\langle\alpha\rangle$-values is oversimplified. The model only considers the ground and first excited states. In our opinion this could explain the increasing deviation between computed and extrapolated $\langle\alpha\rangle$-values at longer chain-length.

The chain length dependence of the components α_{ii} and the associated average polarizability $\langle\alpha\rangle$ and polarizability anisotropy $\Delta\alpha$ are reported in Figs. 8 and 9, respectively. Fig. 8 shows that there is a large non-linear increase of the longitudinal polarizability α_{yy}. In the other directions the evolution of the corresponding polarizability α_{xx} and α_{zz}, respectively, increases linearly with the size of the oligomer. As a consequence, the average polarizability $\langle\alpha\rangle$ and the polarizability anisotropy $\Delta\alpha$ are dominated by the longitudinal component α_{yy}, which is illustrated in Fig. 9. The order of the heterocyclic five-membered π-conjugated oligomers according to the increase in average polarizability $\langle\alpha\rangle$ going from monomers to hexamers is computed as follows: Py = Fu < Th ≈ Pl Ph < Cp < Ph < Si. This calculated sequence can be interpreted by taking two factors into account. The first implies the heteroatom electronegativity, which is larger for first row heteroatoms (N = 3.0, O = 3.5) than for the second row ones (Si = 1.8, P = 2.1, S = 2.5). Therefore electrons are more tightly bound to first-row heteroatoms, which make it more difficult to polarize their electrons. The second factor deals
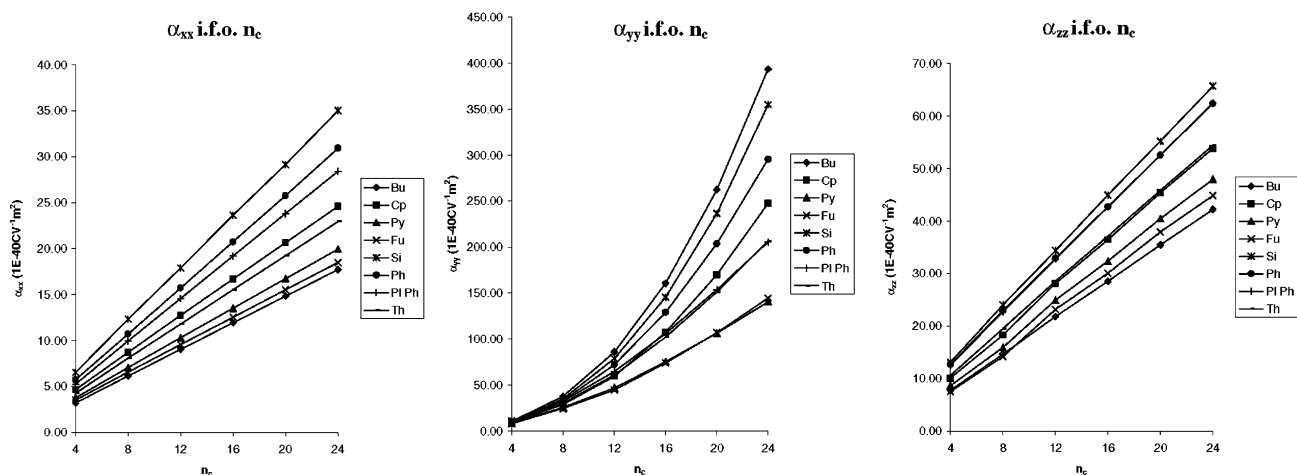
Fig. 8 Chain-length dependence of α_{xx}, α_{yy} and α_{zz} at B3LYP/SV(P) level.

with the building block aromaticity. Since oligomers built from non-aromatic heterocycles are characterized by lower E_g (see the section Energy gaps and vertical ionization energies) and more pronounced linear π-conjugation (see section Oligomers), we expect those π-conjugated systems to possess larger polarizabilities as compared to their aromatic counterparts. If roughly assuming that the most important contribution to α comes from the HOMO → LUMO transition, eqn. (3) will be reduced to eqn. (6)

$$\alpha = \frac{f(r)}{E_g^2} \qquad (6)$$

where $f(r)$ represents the oscillator strength of the HOMO → LUMO transition. Since the building block aromaticity has no significant effect on $f(r)$ (see Tables 4 and 5), we can conclude from eqn. (6) that the smaller the E_g the greater the polarizability.

The electronic polarizability can also be interpreted in terms of the fluctuations in the instantaneous electric dipole moment of the molecule. Thus, the larger the linear π-conjugation (electron delocalization along the oligomer chain) could be, the larger the polarizability of linear π-conjugated systems.
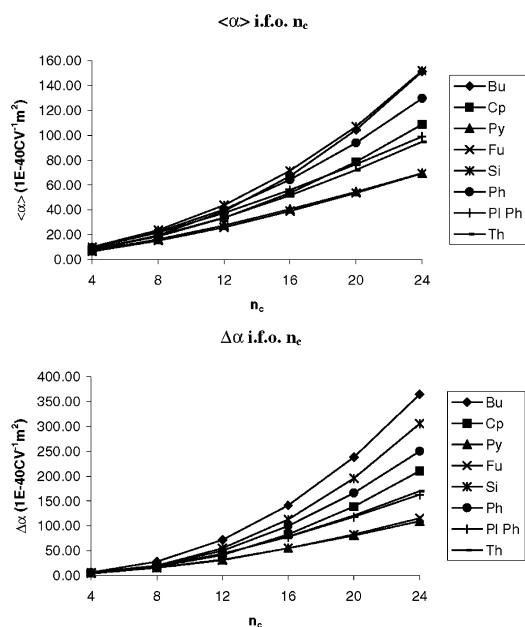
In summary, the order of the average polarizability for heterocyclic five-membered π-conjugated oligomers can be interpreted in broad terms as: aromatic/first row (Py, Fu) < aromatic/second row (Th, Pl Ph) < non-aromatic/first row (Cp) < non-aromatic/second row (Ph, Si).

Conclusions

In this work, computations have shown that oligomers built from non-aromatic five-membered heterocycles are characterized by lower energy gaps compared to oligomers built from aromatic heterocycles. For the vertical ionization energies such correlation was not found. This can be explained by considering the frontier orbitals of both aromatic and non-aromatic heterocyclic oligomers. Out of this consideration, it can be established that the HOMO orbital energies are not influenced by the building block aromaticity. On the contrary, the LUMO orbitals are and become more destabilized for the aromatic heterocyclic oligomers.

Our results also point out that oligomers built from non-aromatic heterocycles are characterized by larger static polarizability tensors compared to their aromatic counterparts. This can be seen as a consequence of the smaller energy gaps non-aromatic heterocycles possess, since molecules become more responsive the closer their frontier orbitals are together.

In the end, we would like to draw the attention towards phosphole, which is to our opinion a promising building block. Results suggest that phosphole oligomers have interesting electronic properties since they are characterized by low energy gaps and large polarizability tensors. Moreover, phosphole possesses a heteroatom which retains a versatile reactivity.[38] This may offer the possibilty of tuning the electronic properties of phosphole oligomers by chemical modifications. For example, bulky substituents at the phosphorus atom can reduce the pyramidality of the tricoordinate phosphorus (σ^3-P) in the phosphole monomer.[39] Some alkylarylphospholes[40] even become aromatic, although they are not completely planar, due to the strong interaction between the phosphorus lone-pair (n_P) and the 1,3-butadiene system. Such control of the aromaticity in the phosphole rings could allow fine-tuning of the electronic properties of the corresponding phosphole oligomers.

Fig. 9 Chain-length dependence of $\langle\alpha\rangle$ and $\Delta\alpha$ at B3LYP/SV(P) level.

References

1 (*a*) J. M. André, J. Delhalle and J. L. Brédas, in *Quantum Chemistry Aided Design of Organic Polymers*, World Scientific, Singapore, 1991; (*b*) J. G. Killian, B. M. Coffey, F. Gao, T. O. Poehler and P. C. Searson, *J. Electrochem. Soc.*, 1996, **143**(3), 936; (*c*) J. L. Brédas, C. Adant, P. Tackx and A. Persoons, *Chem. Rev.*, 1994, **94**, 243; (*d*) P. Prasad and D. Williams, in *Introduction to Nonlinear Optical Effects in Molecules and Polymers*, John Wiley & Sons, New York, p. 199; (*e*) H. Okawa, T. Wada, A. Yamada and H. Sasabe, *Mater. Res. Soc. Symp. Proc.*, 1991, **214**, 23; (*f*) A. Dodabalapur, L. Torsi and H. E. Katz, *Science*, 1995, **268**, 270.
2 (*a*) J. Shinar, S. Ijadi-Maghsoodi, Q. X. Ni, Y. Pang and T. J. Barton, *Synth. Met.*, 1989, **28**, C593; (*b*) T. J. Barton, S. Ijadi-Maghsoodi and Y. Pang, *Macromolecules*, 1991, **24**, 1252.
3 S. Yamaguchi, R. Z. Jin, Y. Itami, T. Goto and K. Tamao, *J. Am. Chem. Soc.*, 1999, **121**, 10 420.
4 (*a*) M. O. Bevierre, F. Mercier, L. Ricard and F. Mathey, *Bull. Soc. Chim. Fr.*, 1992, **129**, 1; (*b*) F. Mathey, *J. Organomet. Chem.*, 1994, **475**, 25; (*c*) E. Deschamps, L. Ricard and F. Mathey, *Angew. Chem.*, 1994, **106**, 11; (*d*) S. Holand, F. Gandolfo, L. Ricard and F. Mathey, *Bull. Soc. Chim. Fr.*, 1996, **133**, 33; (*e*) C. Hay, D. Le Vilain, V. Deborde, L. Toupet and R. Réau, *Chem. Commun.*, 1999, 345; (*f*) C. Hay, C. Fischmeister, M. Hissler, L. Toupet and R. Réau, *Angew. Chem.*, 2000, **112**(10), 1882.
5 T. Jürimäe, M. Strandberg, M. Karelson and J.-L. Calais, *Int. J. Quantum Chem.*, 1995, **54**, 369.
6 U. Salzner, J. B. Lagowski, P. G. Pickup and R. A. Poirier, *Synth. Met.*, 1998, **96**, 177.
7 S. Yamaguchi, Y. Itami and K. Tamao, *Organometallics*, 1998, **17**, 4910.
8 S. Y. Hong, S. J. Kwon and S. C. Kim, *J. Chem. Phys.*, 1995, **103**(5), 1871.
9 A. Hinchliffe, J. Humberto and M. Soscún, *J. Mol. Struct.* (*THEOCHEM*), 1995, **331**, 109.
10 R. G. Parr and W. Yang, in *Density-Functional Theory of Atoms and Molecules*, Oxford University Press, New York, 1989.
11 R. Bauernschmitt and R. Ahlrichs, *Chem. Phys. Lett.*, 1996, **256**, 454.
12 R. Ahlrichs, M. Bär, M. Häser, H. Horn and C. Kölmel, *Chem. Phys. Lett.*, 1989, **162**, 165.
13 M. J. Frisch, G. W. Trucks, H. B. Schlegel, G. E. Scuseria, M. A. Robb, J. R. Cheeseman, V. G. Zakrzewski, J. A. Montgomery, J. A. Montgomery, Jr., R. E. Stratmann, J. C. Burant, S. Dapprich, J. M. Millam, A. D. Daniels, K. N. Kudin, M. C. Strain, O. Farkas, J. Tomasi, V. Barone, M. Cossi, R. Cammi, B. Mennucci, C. Pomelli, C. Adamo, S. Clifford, J. Ochterski, G. A. Petersson, P. Y. Ayala, Q. Cui, K. Morokuma, D. K. Malick, A. D. Rabuck, K. Raghavachari, J. B. Foresman, J. Cioslowski, J. V. Ortiz, B. B. Stefanov, G. Liu, A. Liashenko, P. Piskorz, I. Komaromi, R. Gomperts, R. L. Martin, D. J. Fox, T. Keith, M. A. Al-Laham, A. Peng, C. Y. Nanayakkara, C. Gonzalez, M. Challacombe, P. M. W. Gill, B. Johnson, W. Chen, M. W. Wong, J. L. Andres, C. Gonzalez, M. Head-Gordon, E. S. Replogle and J. A. Pople, Gaussian 98, Revision A.5, Gaussian, Inc., Pittsburgh PA, 1998.
14 C. Van Caillie and R. D. Amos, *Chem. Phys. Lett.*, 2000, **328**, 446.
15 P. v. R. Schleyer, C. Maerker, A. Dransfeld, H. Jiao and N. J. R. v. E. Hommes, *J. Am. Chem. Soc.*, 1996, **118**, 6317.
16 A. Szabo and N. S. Ostlund, *Modern Quantum Chemistry: Introduction to advanced electronic structure theory*, MacMillan Publ. Co., New York, 1982, p. 128.
17 D. Delaere, A. Dransfeld, M. T. Nguyen and L. G. Vanquickenborne, *J. Org. Chem.*, 2000, **65**, 2631.
18 A. Julg and P. François, *Theor. Chim. Acta* (*Berlin*), 1967, **7**, 249.
19 P. v. R. Schleyer, P. K. Freeman, H. Jiao and B. Goldfuss, *Angew. Chem. Int. Ed. Engl.*, 1995, **34**(3), 337.
20 (*a*) E. A. Reed, R. B. Weinstock and F. Weinhold, *J. Chem. Phys.*, 1985, **83**, 735; (*b*) E. A. Reed and F. Weinhold, *J. Chem. Phys.*, 1985, **83**, 1736; (*c*) E. A. Reed, L. A. Curtiss and F. Weinhold, *Chem. Rev.*, 1988, **88**, 899.
21 W. Schäfer, A. Schweig and F. Mathey, *J. Am. Chem. Soc.*, 1976, **98**(2), 407.
22 G. Zotti, S. Martina, G. Wegner and A.-D. Schlüter, *Adv. Mater.*, 1992, **4**, 798.
23 D. Birnbaum and B. E. Kohler, *J. Chem. Phys.*, 1991, **95**(7), 4783.
24 D. Birnbaum and B. E. Kohler, *J. Chem. Phys.*, 1989, **90**(7), 3506.
25 D. Birnbaum and B. E. Kohler, *J. Chem. Phys.*, 1992, **96**(1), 165.
26 R. Colditz, D. Grebner, M. Helbig and S. Rentsch, *Chem. Phys.*, 1995, **201**, 309.
27 G. Horowitz, S. Romdhane, H. Bouchriha, P. Delannoy, J.-L. Monge, F. Kouki and P. Valat, *Synth. Met.*, 1997, **90**, 187.
28 U. Salzner, J. B. Lagowski, P. G. Pickup and R. A. Poirier, *J. Phys. Chem. A*, 1998, **102**, 2572.
29 G. D. Wilett and T. Baer, *J. Am. Chem. Soc.*, 1980, **102**, 6774.
30 M. Bajic, K. Humski, L. Klasinc and B. Ruscic, *Z. Naturforsch., B*, 1985, **40**, 1214.
31 A. Kraak and H. Wynberg, *Tetrahedron*, 1968, **24**, 3881.
32 L. Nyulászi, Gy. Keglevich and L. D. Quin, *J. Organomet. Chem.*, 1996, **61**, 7808.
33 L. Nyulászi, L. Soós and Gy. Keglevich, *J. Organomet. Chem.*, 1998, **566**, 29.
34 B. Champagne, D. H. Mosley and J.-M. André, *J. Chem. Phys.*, 1994, **100**(3), 2034.
35 M. T. Zhao, B. P. Singh and P. N. Prasad, *J. Chem. Phys.*, 1988, **89**, 5535.
36 B. Champagne, E. A. Perpète, S. J. A. van Gisbergen, E.-J. Baerends, J. G. Snijders, C. Soubra-Ghaoui, K. A. Robins and B. Kirtman, *J. Chem. Phys.*, 1998, **109**(23), 10 489.
37 Y. Luo, K. Ruud, P. Norman, D. Jonsson and H. Ågren, *J. Phys. Chem. B.*, 1998, **102**, 1710.
38 (*a*) F. Mathey, *Chem. Rev.*, 1986, **88**, 429; (*b*) D. B. Chesnut and L. Quin, *J. Am. Chem. Soc.*, 1994, **116**, 9638.
39 (*a*) L. Nyulászi, *Tetrahedron*, 2000, **56**, 79; (*b*) L. Nyulászi, *Chem. Rev.*, 2001, **101**, 1229.
40 (*a*) L. Nyulászi, Gy. Keglevich and L. D. Quin, *J. Organomet. Chem.*, 1996, **61**, 7808; (*b*) L. Nyulászi, L. Soós and Gy. Keglevich, *J. Organomet. Chem.*, 1998, **566**, 29.